

# Probabilistic Seismic Hazard Analysis Assessment in Cianjur Following the $M_w$ 5.6, 2022 Earthquake

Yusufa Kholifa Ardha<sup>1</sup>, Iman Satyarno<sup>1\*</sup>, Gayatri Indah Marliyani<sup>2</sup>

<sup>1</sup>Department of Civil and Environmental Engineering, Universitas Gadjah Mada, Yogyakarta, INDONESIA

<sup>2</sup>Department of Geological Engineering, Universitas Gadjah Mada, Yogyakarta, INDONESIA

\*Corresponding author: [imansatyarno@ugm.ac.id](mailto:imansatyarno@ugm.ac.id)

SUBMITTED 31 December 2024 REVISED 17 May 2025 ACCEPTED 19 May 2025

**ABSTRACT** On November 21, 2022, a  $M_w$  5.6 earthquake struck Cianjur, West Java, Indonesia, causing extensive damage to buildings, infrastructure, and public facilities, and resulting in 602 fatalities and thousands of injuries. The earthquake's hypocenter was located near the Cugenang Sub-District, leading to the identification of the previously unmapped Cugenang Fault as its source. This discovery highlights the need to reassess seismic hazards in the region, as it reveals the existence of previously unrecognized active faults. This study conducts a probabilistic seismic hazard analysis (PSHA) for Cianjur using an updated seismic source model that incorporates the Cugenang Fault. We apply updated ground motion prediction equations (GMPEs) and utilize the logic tree method to account for uncertainties in attenuation equations and source parameters. Ground motion is expressed as peak ground acceleration (PGA) on both bedrock and surface conditions for return periods of 100, 150, 250, 500, 1,000, 2,500, 5,000, and 10,000 years. These return periods capture the hazard levels associated with both frequent low-magnitude and rare high-magnitude earthquakes. Our findings indicate that high PGA values in the Cianjur area are concentrated around crustal faults, exceeding 1.0 g for return periods of 2,500 years and beyond. The Cugenang Fault has a localized impact, with its influence extending up to approximately 10 km from the fault line. A seismic hazard disaggregation analysis confirms that crustal faults are the dominant seismic sources in the region. The results of this study provide valuable insights for updated seismic risk in Cianjur and support future mitigation strategies, urban planning, and infrastructure design to enhance earthquake resilience in the affected area.

**KEYWORDS** Probabilistic seismic hazard analysis, Cianjur, peak ground acceleration, Cugenang Fault

© The Author(s) 2025. This article is distributed under a Creative Commons Attribution-ShareAlike 4.0 International license.

## 1 INTRODUCTION

On November 21, 2022, Cianjur and neighboring areas were hit by an  $M_w$  5.6 earthquake, with the hypocenter located inland at a depth of 10 km. According to a report from the Cianjur Regional Disaster Management Agency (BPBD), the earthquake caused severe damage, resulting in 602 fatalities and over 56,000 damaged buildings. Among the damaged structures were critical public facilities, including 700 schools and 18 medical centers. The shallow depth of the hypocenter was a significant factor contributing to the extensive destruction (Kramer and Stewart, 2024). However, discussion emerged because the epicenter was located approximately 10 km from the nearest mapped fault, suggesting that the event may have originated from an unmapped source (Supendi et al., 2023). Historically, Cianjur experienced a major earthquake in 1834 with an estimated intensity of VIII – IX on the Modified Mercalli Intensity scale (Setiyono et al., 2019). However, due to the absence of seismological instruments at that time, the precise location and depth of its hypocenter remain unknown. Aside from this event and the 2022 earthquake, no other significant shallow earthquakes have been recorded in the Cianjur Region (see Figure 1).

Cianjur is situated within a volcanic arc formed by the subduction of the Australian Plate beneath the Eurasian Plate (Hall and Spakman, 2015). This tectonic activity has produced several active crustal faults in the region, including the Cimandiri Fault (Marliyani et al., 2016), the Lembang Fault (Daryono et al., 2019), and the Baribis Fault (Aribowo et al., 2022). Supendi et al. (2023) analyzed the source of the 2022 Cianjur earthquake using seismic wave data. They determined that it originated from a conjugate fault composed of two segments oriented in North-Northwest – South-Southeast (NNW – SSE) and West-Southwest – East-Northeast (WSW – ENE) directions. This fault was subsequently named the Cugenang Fault, as it is located in the Cugenang Sub-District (Supendi et al., 2023). The slipping along of these faults could generate a tectonic earthquake (Maheswari, 2024).

Cianjur District consists of 32 sub-districts and has a total population of 2,535,002 people, with Cianjur Sub-District being the most densely populated area (BPS-Statistics of Cianjur Regency, 2024). The majority of the district's population is concentrated in the northern region, which is characterized by flat terrain. This

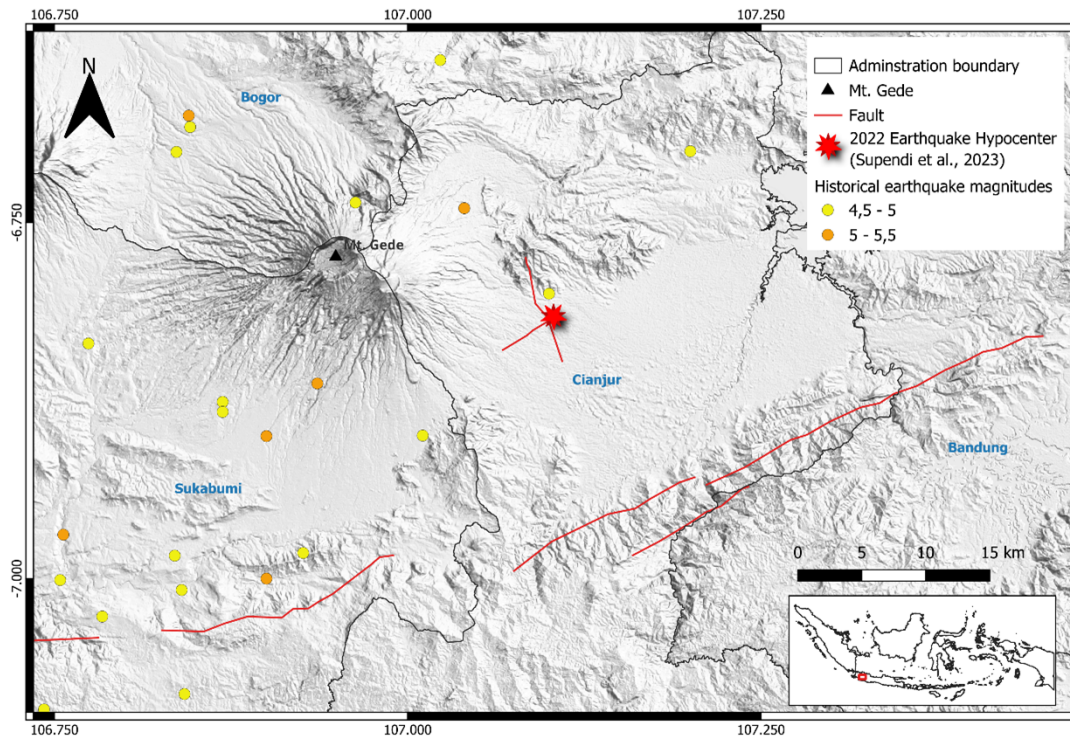


Figure 1 Seismic activity records around Cianjur for shallow earthquakes (<50 km) with significant magnitudes (>M4.5) from January 1900 – 22 November 2022. Seismic data based on BMKG repository catalogue, USGS earthquake catalogue and the IRIS earthquake browser. The red star represents hypocenter of 2022 earthquake (Supendi et al., 2023). Red lines represent fault lines (Marliyani et al., 2016; Supendi et al., 2023). Basemap based on DEMNAS (<https://tanahair.indonesia.go.id>).

area is located near the Cugenang Fault (see Figure 1), making it essential to reassess the seismic hazard level to ensure that appropriate mitigation measures are in place.

Probabilistic seismic hazard analysis (PSHA) is used to estimate seismic hazard by assessing the probability of earthquake occurrence and magnitude over specific return periods. This method aids in optimizing the balance between cost, performance, and risk in engineering design (Cornell, 1968). A previous study conducted by the National Centre for Earthquake Study (PUSGEN) produced a national-scale seismic hazard map (Widiyantoro et al., 2022), while Damanik et al. (2023) developed a seismic hazard map specifically for West Java, which includes Cianjur. However, neither study accounted for the Cugenang Fault as an earthquake source. This study evaluates seismic hazard in Cianjur by incorporating all known earthquake sources across multiple return periods. We consider eight return periods: 100, 150, 250, 500, 1,000, 2,500, 5,000, and 10,000 years. Shorter return periods, such as 150 years, are applicable to residential and everyday infrastructure, including roads, while a 1,000-year return period is typically used for bridge infrastructure (SNI 2833:2016). The 2,500-year return period is designated for critical infrastructure (SNI 1726:2019). Longer return periods, such as 5,000 and 10,000 years, are used for structures where failure would lead to catastrophic consequences, such as nuclear facilities (Bommer et al.,

2011). Earthquake ground motion is quantified as peak ground acceleration (PGA) at both bedrock and surface levels, accounting for local site conditions.

## 2 DATA

### 2.1 Seismic Source Characterization

Seismic sources capable of generating ground motion in the study area include subduction interfaces, crustal faults, and background seismicity. The subduction interface source model represents earthquakes occurring at the boundary of the subduction zone. For this study, a depth limit of 50 km is applied to the subduction interface source model, while deeper seismicity within the Benioff zone is represented by a deep background source model (Asrurifak et al., 2010). The Java Megathrust results from the subduction of the Australian Plate beneath the Eurasian Plate (Hall and Spakman, 2015). It is divided into three segments: the Sunda Strait, West-Central Java, and East Java Megathrust, with an estimated maximum magnitude of  $M_w$  8.8 (Irsyam et al., 2017). Historical earthquakes along the West Java segment include the tsunamigenic events of 2006 and 2009, which had magnitudes of  $M_w$  6.8 and  $M_w$  7.3, respectively (Setiyono et al., 2019). The detailed seismic parameters used in this study, including fault geometry, slip rates, and Gutenberg-Richter values, are listed in Table 1.

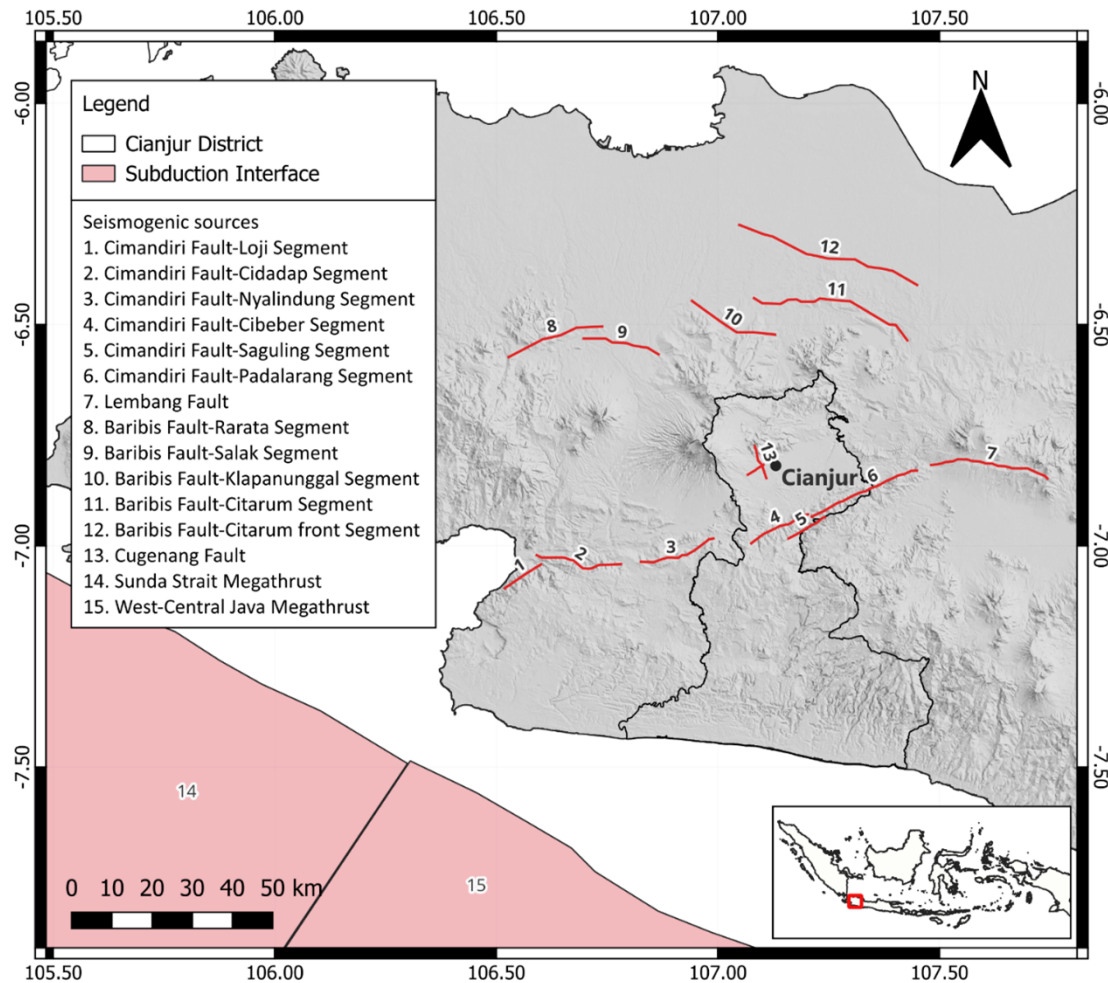


Figure 2 Map of seismic sources in the study area. Black dot represents the capital of Cianjur District. Red lines indicate fault lines. Fault numbered 1 – 6 are segments of the Cimandiri Fault (Marliyani et al., 2016), Fault numbered 7 is the Lembang Fault (Daryono et al., 2019); Fault numbered 8 – 12 are segments of the Baribis Fault System (Aribowo et al., 2022), Fault numbered 13 is the Cugenang Fault (Supendi et al., 2023). Area shaded red are subduction interface 14) Sunda Strait Megathrust and 15) West-Central Java Megathrust (Widiyantoro et al., 2022). Basemap based on DEMNAS (<https://tanahair.indonesia.go.id>).

Crustal faults within a 250 km radius of the study area are also considered seismic sources (Irsyam et al., 2015). As shown in Figure 2, these include the Cimandiri Fault (Marliyani et al., 2016), the Baribis Fault (Aribowo et al., 2022), the Lembang Fault (Daryono et al., 2019), and the newly identified Cugenang Fault (Supendi et al., 2023). Key parameters for assessing seismic hazard from these faults include slip rates, estimated maximum magnitudes, and fault geometry (see Table 1). Fault geometry consists of fault length, dip angle, and the depth of the seismogenic layer. The seismogenic layer, which is the brittle portion of a fault capable of nucleating earthquakes, has depth boundaries that define its upper and lower limits (Scholz, 2019). In this study, the top and bottom depths of the seismogenic layer are based on previous studies (Irsyam et al., 2017; Supendi et al., 2023). Other fault parameters used in this study are derived from previous research: Cimandiri Fault has a length ranging from 9.6 to 21 km with  $60^\circ$  dip and slip rate ranging from 0.1 to 0.5 mm/year (Marliyani et al., 2016), Lembang Fault has

a length of 29 km with  $75^\circ$  dip and slip rate of 2 mm/year (Daryono et al., 2019), Baribis Fault has a length ranging from 19 to 48 km with dip  $65^\circ$  (Aribowo et al., 2022) and slip rate of 1.2 mm/year (Damanik et al., 2023), Cugenang Fault length is 8 and 4.6 km with dip  $87^\circ$  and  $69^\circ$  for each segment, respectively (Supendi et al., 2023).

Apart from the 2022 earthquake, no previous seismic activity has been recorded on the Cugenang Fault (Supendi et al., 2023). There are no prior studies investigating its slip rate, so for estimation purposes, we adopt the slip rate of the nearest fault, the Cimandiri Fault, at approximately 0.1 mm/year. This low slip rate is consistent with the limited seismic activity observed on the Cugenang Fault.

The possible maximum magnitudes for the faults are estimated using magnitude-fault length scaling relationships. For most crustal faults, the attenuation model developed by Cheng et al. (2019) is used, as it has been found to produce the smallest misfit for In-

Table 1. Seismic source parameters used in this study

Seismic source name	Segment	Fault type	Dip (°)	Length (km)	Top (km)	Bottom (km)	Slip Rate (mm/year)	$M_{max}$ ( $M_w$ )	GR Parameter $a; b$ value
Cimandiri	Loji	<i>Left-lateral reverse</i>	60	9.6	3	18	0.5	6.5 <sup>a</sup>	-
	Cidadap	<i>Left-lateral reverse</i>	60	21	3	18	0.5	6.9 <sup>a</sup>	-
	Nyalindung	<i>Left-lateral reverse</i>	60	19	3	18	0.4	6.9 <sup>a</sup>	-
	Cibeber	<i>Left-lateral reverse</i>	60	16	3	18	0.4	6.8 <sup>a</sup>	-
	Saguling	<i>Left-lateral strike-slip</i>	60	11	3	18	0.1	6.6 <sup>a</sup>	-
	Padalarang	<i>Left-lateral strike-slip</i>	60	19	3	18	0.1	6.9 <sup>a</sup>	-
Lembang	Lembang	<i>Left-lateral strike-slip</i>	75	29	3	18	2.0	6.4 <sup>b</sup>	-
Baribis	Rarata	<i>Left-lateral strike-slip</i>	90	25	3	18	1.2	6.3 <sup>b</sup>	-
	Salak	<i>Reverse</i>	65	19	3	18	1.2	6.1 <sup>b</sup>	-
	Klapanunggal	<i>Reverse</i>	65	24	3	18	1.2	6.3 <sup>b</sup>	-
	Citarum	<i>Reverse</i>	65	43	3	18	1.2	6.7 <sup>b</sup>	-
	Citarum front	<i>Reverse</i>	65	48	3	18	1.2	6.8 <sup>b</sup>	-
Cugenang	NNW - SSE	<i>Right-lateral strike-slip</i>	87	8	5	15	0.1	6.2 <sup>c</sup>	-
	WSW - ENE	<i>Left-lateral strike-slip</i>	69	4.6	5	15	0.1	5.7 <sup>c</sup>	-
Java	Sunda Strait	<i>Reverse</i>	15	280	-	-	4.0	8.7 <sup>d</sup>	5.99;1.15
Megathrust	West-central Java	<i>Reverse</i>	15	320	-	-	4.0	8.7 <sup>d</sup>	5.55;1.08

$M_{max}$  value based on <sup>(a)</sup>Marliyani et al. (2016), <sup>(b)</sup> magnitude scaling relationship by Cheng et al. (2019),

<sup>(c)</sup> magnitude scaling relationship for slow slip rate (Stirling et al., 2008), <sup>(d)</sup>Irsyam et al. (2017)

Indonesia (Gunawan, 2021). However, since the Cheng et al. (2019) model is not suitable for slow-slip faults (<1 mm/year), the scaling relationship for low slip rate crustal faults by Stirling et al. (2008) is used for the Cugenang Fault. Cugenang Fault has a dip angle 87° and 69° for each segment with a seismicity depth of 10 km (Supendi et al., 2023). Based on this approach, the estimated maximum magnitudes for the Cugenang Fault are  $M_w$  6.2 for NNW – SSE segment and  $M_w$  5.7 for WSW – ENE segment. The maximum magnitude estimation for the Cimandiri Fault is based on Marliyani et al. (2016).

Background seismicity is generally classified by depth into shallow background seismicity (0 – 50 km) and deep background seismicity (50 – 300 km). Shallow background seismicity represents fault-generated earthquakes with magnitudes ranging from  $M_w$  4.5 to 6.5, while deep background seismicity corresponds to subduction intraslab events with magnitudes between  $M_w$  5 and 7.5 (Irsyam et al., 2020). The magnitude-frequency distribution for background seismicity is estimated using the smoothed gridded seismicity method (Frankel, 1995), based on earthquake records from the BMKG, United States Geological Survey (USGS), and the Incorporated Research Institutions for Seismology (IRIS) from January 1, 1900, to August 31, 2024.

## 2.2 Local Site Condition

Shallow geological conditions can either amplify or attenuate earthquake-induced ground motion (Kramer and Stewart, 2024). Seismic site conditions are stan-

dardized by measuring the shear wave velocity in the upper 30 meters of the Earth's surface ( $V_S^{30}$ ). In this study, topographic slope is used as a proxy for  $V_S^{30}$  (Wald and Allen, 2007). Wald and Allen (2007) developed their  $V_S^{30}$  model using topographic data with a resolution of 30 arc seconds. To ensure consistency, we use GMTED2010 topographic data, which also has a resolution of 30 arc seconds, obtained from the United States Geological Survey (USGS) [[https://topotools.cr.usgs.gov/gmted\\_viewer/index.html](https://topotools.cr.usgs.gov/gmted_viewer/index.html)] (Danielson and Gesch, 2011). Seismic site classification follows the National Earthquake Hazards Reduction Program (NEHRP) site class system, which categorizes ground motion response based on  $V_S^{30}$  values (Borcherdt, 1994). This classification is used to estimate ground motion at various locations within the study area.

## 3 METHOD

### 3.1 Ground Motion Prediction Equation

Engineering design requires objective and quantitative assessments of ground motion generated by earthquakes. To predict ground motion, ground motion prediction equations (GMPEs) are used, which are derived from historical earthquake data (Baker et al., 2021). Currently, no region-specific GMPEs have been developed for Java or Indonesia; therefore, the selection of GMPEs in this study is based on tectonic and geological similarities with other regions where they have been developed. This study considers three types of seismo-

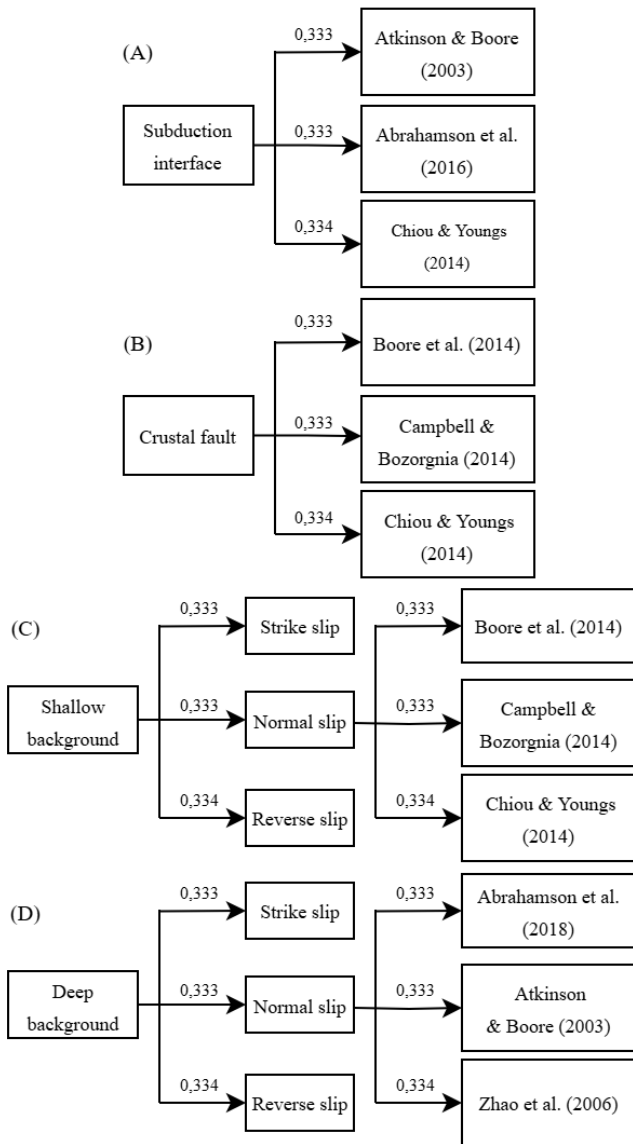


Figure 3 Logic tree used for seismic hazard calculation for (A) subduction interface, (B) crustal fault, (C) shallow background, and (D) deep background seismic source.

genic sources: subduction interface, crustal fault, and subduction intraslab. GMPEs for the subduction interface seismogenic source using equations from Atkinson and Boore (2003), Abrahamson et al. (2016) and Zhao et al. (2006). GMPEs for the crustal fault seismogenic source from Boore et al. (2014), Campbell and Bozorgnia (2014) and Chiou and Youngs (2014). GMPEs for the subduction intraslab seismogenic source from Abrahamson et al. (2018), Atkinson and Boore (2003) and Zhao et al. (2006). To account for uncertainties in GMPE attenuation and source models, we apply the logic tree method, which allows for the integration of multiple GMPEs in the seismic hazard assessment. The logic tree structure used in this study is presented in Figure 3.

### 3.2 Magnitude Frquency Distribution

Magnitude-frequency distribution (MFD) is a mathematical model that describes the relative likelihoods of all events that can be generated by a particular source or region (Baker et al., 2021). We use two types of MFD to determine seismic hazard. The first MFD expresses the annual frequency of earthquakes on a linear scale in a logarithmic scale with  $a$  and  $b$  parameters, where  $a$  value represents total seismic activity and the  $b$  value represents relative likelihood of small versus large magnitudes (Gutenberg and Richter, 1944). The second MFD are hybrid method that combines parameters from Gutenberg and Richter (1944) with moment rates from Schwartz and Coppersmith (1984) and Youngs and Coppersmith (1986). Gutenberg-Richter MFD is used for background seismicity sources, whereas the hybrid MFD is used for subduction interfaces and crustal fault sources. Seismic hazard calculations are processed using the OpenQuake engine (Pagani et al., 2014) as peak ground acceleration (PGA) with a site spacing of 1 km.

## 4 RESULTS

Ground motion was calculated for return periods of 100, 150, 250, 500, 1,000, 2,500, 5,000, and 10,000 years. Seismic hazard assessment was conducted under two conditions: bedrock ( $V_S^{30} \sim 760$  m/s) and local site conditions. For the bedrock calculations, we used a  $V_S^{30}$  value of 760 m/s, as this represents the lower boundary of Site Class B (rock) according to the NEHRP site classification (Borcherdt, 1994). This value is derived from studies of typical rock site conditions, where  $V_S^{30}$  is consistently measured at 760 m/s. Consequently, a constant  $V_S^{30}$  value of 760 m/s was applied for seismic hazard calculations at bedrock. To identify the dominant seismic sources affecting the study area, seismic hazard disaggregation was performed. The analysis focused on four densely populated sub-districts in Cianjur: Cianjur, Cibeber, Karangtengah, and Cipanas.

### 4.1 Seismic Hazard at Bedrock

Seismic hazard calculations at bedrock assuming a constant  $V_S^{30}$  value at  $\sim 760$  m/s. For a 100-year return period, the mean peak ground acceleration (PGA) ranges from 0.042 to 0.281 g. For a 150-year return period, the mean PGA ranges from 0.060 to 0.405 g. For a 250-year return period, the mean PGA ranges from 0.083 to 0.539 g. For a 500-year return period, the mean PGA ranges from 0.118 to 0.705 g. For a 1,000-year return period, the mean PGA ranges from 0.173 to 0.935 g. For a 2,500-year return period, the mean PGA ranges from 0.261 to 1.233 g. For a 5,000-year return period, the mean PGA ranges from 0.350 to 1.490 g. Finally, for a 10,000-year return period, the mean PGA ranges from 0.460 to 1.700 g (see Figure 4).

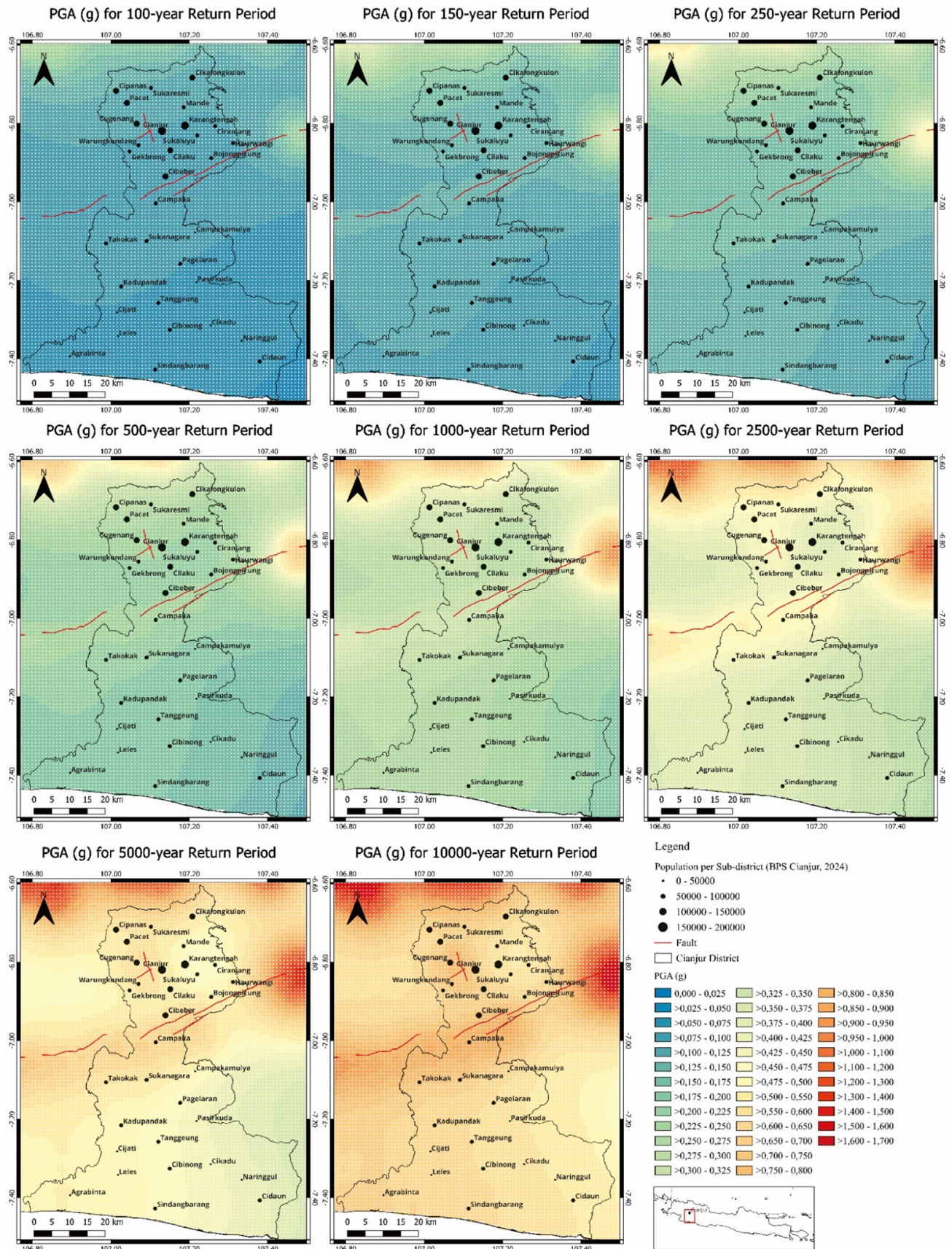


Figure 4 Seismic hazard map at bedrock for respective return periods. The same colour scale is used on each return periods. Red lines represent fault line. Area bordered by black polygons are the Cianjur District. Black dots represent population per sub-districts. Index map showed in the bottom right with a red square indicating the study area.

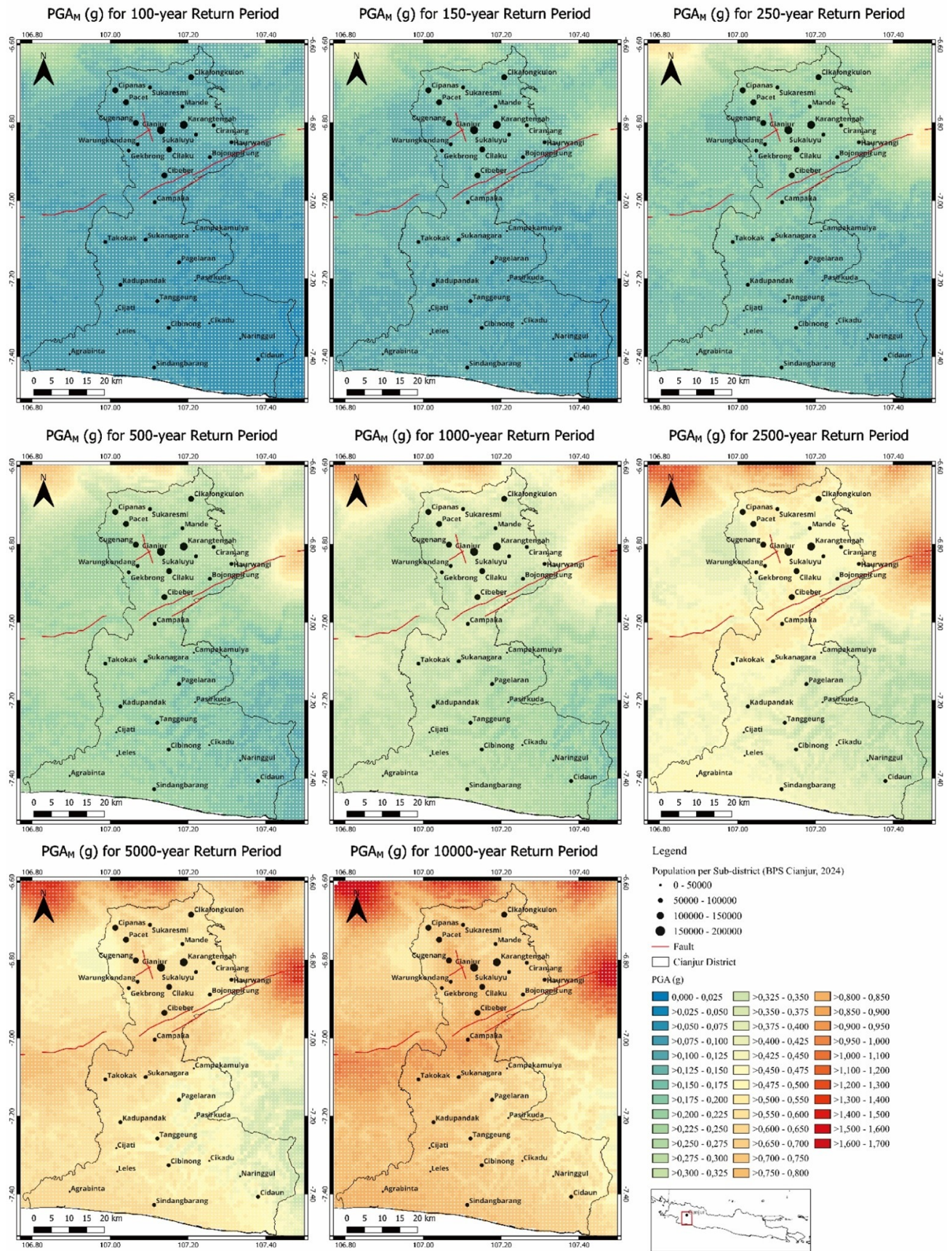


Figure 5 Seismic hazard map with local site conditions for respective return periods. The same colour scale is used on each return periods. Red lines represent fault line. Area bordered by black polygons are Cianjur District. Black dots represent population per sub-districts. Index map is shown in the bottom right with a red square indicating the study area.

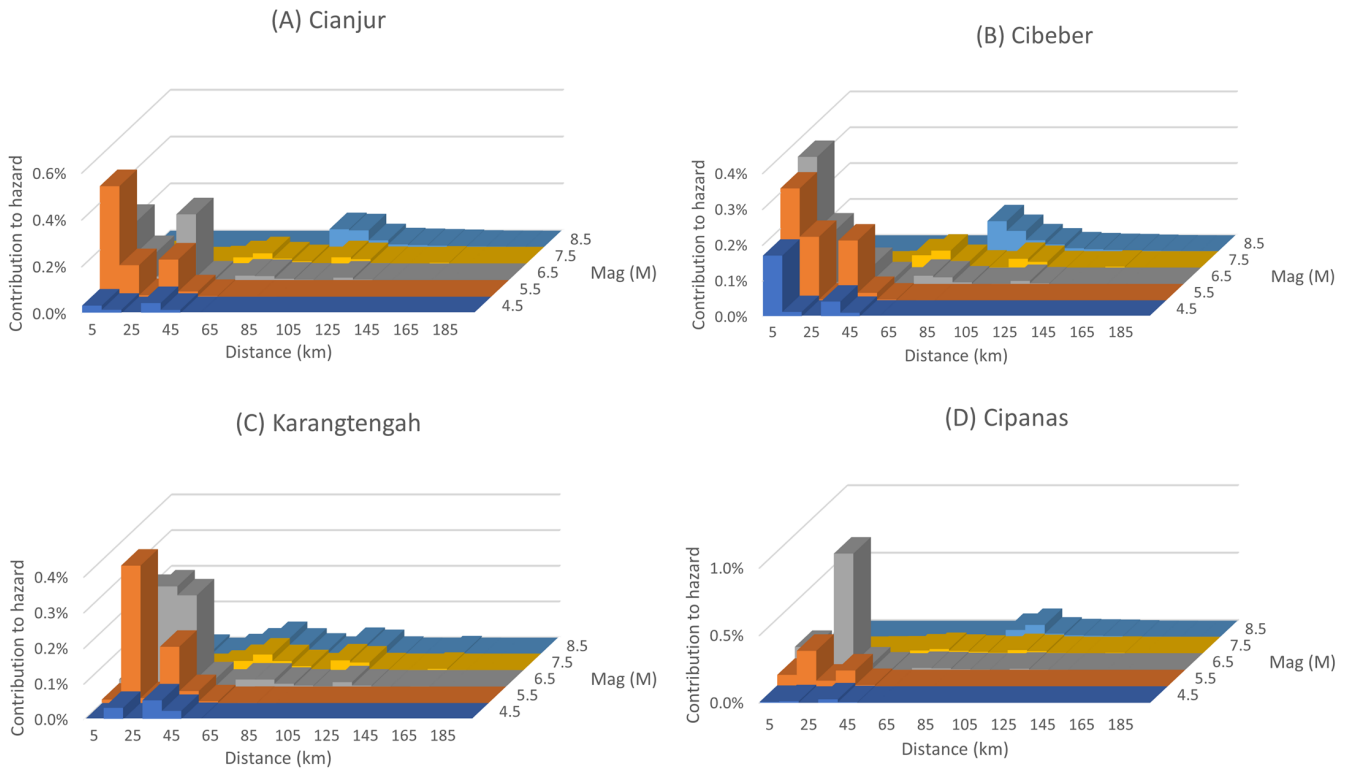


Figure 6 Seismic hazard disaggregation for four sub-districts in Cianjur using a 2,500-year return period: (A) Cianjur Sub-District, (B) Cibeber Sub-District, (C) Karangtengah Sub-District, and (D) Cipanas Sub-District. Magnitude and distance used as disaggregation parameters to identify the most significant seismic sources.

#### 4.2 Seismic Hazard at Local Site

In this section, seismic hazard calculations are conducted while taking local site conditions into account, and the results are shown in Figure 5. The mean peak ground acceleration with site effects (PGAM) values for various return periods range from 0.041 to 0.326 g for a 100-year return period, 0.059 to 0.453 g for a 150-year return period, 0.080 to 0.592 g for a 250-year return period, 0.113 to 0.771 g for a 500-year return period, 0.163 to 0.988 g for a 1,000-year return period, 0.240 to 1.250 g for a 2,500-year return period, 0.310 to 1.480 g for a 5,000-year return period, and 0.420 to 1.700 g for a 10,000-year return period, as shown in Figure 5. Generally, ground motion at local sites exhibits a lower minimum and a higher maximum PGA value compared to bedrock, due to site-specific amplification and de-amplification effects influenced by geological conditions.

#### 4.3 Seismic Hazard Disaggregation

To identify the dominant seismic sources in the study area, a seismic hazard disaggregation study was conducted for four of the most populated sub-districts in Cianjur: Cianjur, Cibeber, Karangtengah, and Cipanas. The 2,500-year return period was chosen for this anal-

ysis because it provides a representative scenario for large but rare earthquakes. Shorter return periods may not sufficiently capture these significant events, while longer return periods tend to produce excessively high values. Furthermore, the 2,500-year return period is widely used in building codes, including ASCE 7, Eurocode 8, and SNI 1726:2019.

Seismic hazard disaggregation was conducted using earthquake magnitude and seismic source distance as parameters (see Figure 6). The most significant earthquake scenario for the Cianjur Sub-District occurs at a maximum distance of 5 km with a magnitude of  $M_w$  5.5. In the Cibeber Sub-District, the maximum distance is also 5 km, but with a magnitude of  $M_w$  6.5. For Karangtengah Sub-District, the maximum distance is 15 km with a magnitude of  $M_w$  5.5, while in Cipanas Sub-District, the maximum distance is 25 km with a magnitude of  $M_w$  6.5. Given the relatively short distances of these events, all occurring within 25 km, and their moderate magnitudes, the dominant seismic hazard sources in these areas are identified as crustal faults.

## 5 DISCUSSION

The seismic hazard at bedrock exhibits a uniform pattern due to the assumption of a constant  $V_s^{30}$  value of approximately 760 m/s. In contrast, the seismic hazard at local sites varies significantly depending on site-specific conditions. The western part of the Cugenang Sub-District experiences a de-amplification effect due to its mountainous morphology and solid rock composition. Conversely, the central region, which includes the Cianjur, Karangtengah, and Cibeber Sub-Districts, shows an amplification effect due to its flat terrain and loose soil composition. These sub-districts are densely populated, making seismic hazard mitigation especially critical in these areas.

Both the seismic hazard map at bedrock and the local site map indicates high peak ground acceleration (PGA) values along fault lines and in the direction of fault dips. The southern area of the Cimandiri Fault exhibits high PGA values because the fault dips southward. Similarly, the northern part of the study area shows elevated PGA values due to the presence of Baribis Fault segments, which also dip southward. The highest mean PGA values are observed in the eastern region, near the Lembang Fault, across all return periods. This is due to the Lembang Fault's high slip rate ( $\sim 2$  mm/year), which increases the likelihood of large-magnitude earthquakes.

Previous seismic hazard assessments in Cianjur have been conducted by Irsyam et al. (2020) and Damanik et al. (2023). Compared to these studies, our research incorporates the Cugenang Fault as a seismic source and updates the ground motion prediction equations (GMPEs) with newer models. The seismic hazard maps presented in this study show higher PGA values in the northern region due to the addition of Baribis Fault segments, which were not included in the national seismic hazard map (Irsyam et al., 2017; Widiyantoro et al., 2022). Additionally, the area around the Cugenang Fault also exhibits high PGA values starting from the 500-year return period, primarily due to the fault's low slip rate ( $\sim 0.1$  mm/year) and the lack of recorded earthquake activity. The Indonesian seismic hazard maps have been compiled at a national scale (Irsyam et al., 2017; Widiyantoro et al., 2022); consequently, the level of detail is generally low. This paper presents seismic hazard maps at a local scale and introduces a newer source model to provide more precise and relevant results for assessing seismic hazard in the Cianjur area.

Seismic hazard disaggregation analysis was conducted for a 2,500-year return period, which serves as the reference for engineering design loads. The four most populous sub-districts in Cianjur were selected for this analysis. The results indicate that the most significant earthquake events for these sites originate from relatively short distances ( $< 25$  km) and have magnitudes

below  $M_w$  6.5. This suggests that crustal faults are the dominant seismic hazard source. Specifically, Cianjur, Karangtengah, and Cipanas Sub-Districts are most affected by the Cugenang Fault, while the Cibeber Sub-District is primarily influenced by the Cimandiri Fault. Our findings highlight that the Cugenang Fault poses the most significant seismic hazard to three of the most densely populated sub-districts in Cianjur. We hope that these results provide valuable insights into the micro-scale seismic hazards posed by the Cugenang Fault and contribute to more effective seismic risk mitigation in the Cianjur District.

## 6 CONCLUSION

This study assesses the seismic hazard in Cianjur and its surrounding areas by analyzing peak ground acceleration (PGA) at both bedrock and local sites using the OpenQuake engine. Topographic slope data was used to estimate  $V_s^{30}$  values, which were classified based on NEHRP site classes. The fault seismic source model includes the latest identified Cugenang Fault, which was responsible for the 2022 Cianjur earthquake.

The seismic hazard maps indicate that the distribution of ground motion follows the pattern of fault strikes. The highest mean PGA values are concentrated around the Lembang Fault, while the Cugenang Fault has a more localized impact near the rupture area. Seismic source disaggregation analysis was conducted for the four most populated sub-districts in Cianjur: Cianjur, Karangtengah, Cibeber, and Cipanas. The results confirm that crustal faults are the primary seismic sources, with the Cugenang Fault and Cimandiri Fault being the closest sources to Cianjur.

Compared to the 2017 and 2022 Indonesian seismic hazard maps, this study provides a more detailed assessment, showing a wider range of ground motion values, including both a lower minimum and a higher maximum PGA. These findings contribute to a better understanding of seismic hazards in Cianjur, thereby supporting more effective earthquake mitigation strategies and infrastructure planning.

## DISCLAIMER

The authors declare no conflict of interest.

## REFERENCES

- Abrahamson, N., Gregor, N. and Addoc, K. (2016), 'BC Hydro Ground Motion Prediction Equations For Subduction Earthquakes', *Earthquake Spectra* **32**(1), 23–44. URL: <https://doi.org/10.1193/051712EQS188MR>
- Abrahamson, N., Kuehn, N., Gulerce, Z., Gregor, N.,

- Bozorgnia, Y., Chiou, B., Idriss, I. M., Campbell, K., Youngs, R., Parker, G. and Stewart, J. (2018), 'Update of the BC Hydro Subduction Ground-Motion Model using the NGA-Subduction Dataset', *PEER Reports* **2018-02**.  
**URL:** <https://doi.org/10.55461/OYCD7434>
- Aribowo, S., Husson, L., Natawidjaja, D. H., Authemayou, C., Daryono, M. R., Puji, A., Valla, P., Pamumpuni, A., Wardhana, D., de Gelder, G., Djarwadi, D. and Lorcery, M. (2022), 'Active Back-Arc Thrust in North West Java, Indonesia', *Tectonics* **41**(7).  
**URL:** <https://doi.org/10.1029/2021TC007120>
- Asrurifak, M., Irsyam, M., Budiono, B., Triyoso, W. and Hendriyawan. (2010), 'Development of Spectral Hazard Map for Indonesia with a Return Period of 2500 Years using Probabilistic Method', *Civil Engineering Dimension* **12**(1), 52–62.  
**URL:** <https://doi.org/10.9744/ced.12.1.52-62>
- Atkinson, G. M. and Boore, D. M. (2003), 'Empirical ground-motion relations for subduction-zone earthquakes and their application to Cascadia and other regions', *Bulletin of the Seismological Society of America* **93**(4), 1703–1729.  
**URL:** <https://doi.org/10.1785/0120020156>
- Baker, J. W., Bradley, B. A. and Stafford, P. J. (2021), *Seismic Hazard and Risk Analysis*, Cambridge: Cambridge University Press.  
**URL:** <https://doi.org/10.1017/9781108425056>
- Bommer, J. J., Papaspiliou, M. and Price, W. (2011), 'Earthquake response spectra for seismic design of nuclear power plants in the UK', *Nuclear Engineering and Design* **241**(3), 968–977.  
**URL:** <https://doi.org/10.1016/j.nucengdes.2011.01.029>
- Boore, D. M., Stewart, J. P., Seyhan, E. and Atkinson, G. M. (2014), 'NGA-West2 equations for predicting PGA, PGV, and 5  
**URL:** <https://doi.org/10.1193/070113EQS184M>
- Borcherdt, R. D. (1994), 'Estimates of Site-Dependent Response Spectra for Design (Methodology and Justification)', *Earthquake Spectra* **10**(4), 617–653.  
**URL:** <https://doi.org/10.1193/1.1585791>
- BPS-Statistics of Cianjur Regency (2024), 'Cianjur Regency in Figures 2024'.
- Campbell, K. W. and Bozorgnia, Y. (2014), 'NGA-West2 ground motion model for the average horizontal components of PGA, PGV, and 5  
**URL:** <https://doi.org/10.1193/062913EQS175M>
- Cheng, J., Rong, Y., Magistrale, H., Chen, G. and Xu, X. (2019), 'Earthquake rupture scaling relations for mainland China', *Seismological Research Letters* **91**(1), 248–261.  
**URL:** <https://doi.org/10.1785/0220190129>
- Chiou, B. S. J. and Youngs, R. R. (2014), 'Update of the Chiou and Youngs NGA model for the average horizontal component of peak ground motion and response spectra', *Earthquake Spectra* **30**(3), 1117–1153.  
**URL:** <https://doi.org/10.1193/072813EQS219M>
- Cornell, C. A. (1968), 'Engineering Seismic Risk Analysis', *Bulletin of the Seismological Society of America* **58**(5), 1583–1606.  
**URL:** <https://doi.org/10.1785/BSSA0580051583>
- Damanik, R., Gunawan, E., Widiyantoro, S., Supendi, P., Atmaja, F. W., Ardianto, Husni, Y. M., Zulfakriza and Sahara, D. P. (2023), 'New assessment of the probabilistic seismic hazard analysis for the greater Jakarta area, Indonesia', *Geomatics, Natural Hazards and Risk* **14**(1).  
**URL:** <https://doi.org/10.1080/19475705.2023.2202805>
- Danielson, J. J. and Gesch, D. B. (2011), 'Global Multi-resolution Terrain Elevation Data 2010 (GMTED2010)', U.S. Geological Survey Open-File Report 2011-1073. [http://eros.usgs.gov/#/Find\\_Data/Products\\_and\\_Data\\_Available/GMTED2010](http://eros.usgs.gov/#/Find_Data/Products_and_Data_Available/GMTED2010).
- Daryono, M. R., Natawidjaja, D. H., Sapiie, B. and Cummins, P. (2019), 'Earthquake Geology of the Lembang Fault, West Java, Indonesia', *Tectonophysics* **751**, 180–191.  
**URL:** <https://doi.org/10.1016/j.tecto.2018.12.014>
- Frankel, A. (1995), 'Mapping seismic hazard in the central and eastern United States', *Seismological Research Letters* **66**(4), 8–21.  
**URL:** <https://doi.org/10.1785/gssrl.66.4.8>
- Gunawan, E. (2021), 'An assessment of earthquake scaling relationships for crustal earthquakes in Indonesia', *Seismological Research Letters* **92**(4), 2490–2497.  
**URL:** <https://doi.org/10.1785/0220200267>
- Gutenberg, B. and Richter, C. F. (1944), 'Frequency of Earthquakes in California', *Bulletin of the Seismological Society of America* **34**(4), 185–188.  
**URL:** <https://doi.org/10.1785/BSSA0340040185>
- Hall, R. and Spakman, W. (2015), 'Mantle structure and tectonic history of SE Asia', *Tectonophysics* **658**, 14–45.  
**URL:** <https://doi.org/10.1016/j.tecto.2015.07.003>
- Irsyam, M., Cummins, P. R., Asrurifak, M., Faizal, L., Natawidjaja, D. H., Widiyantoro, S., Meilano, I., Triyoso, W., Rudiyanto, A., Hidayati, S., Ridwan, M., Hanifa, N. R. and Syahbana, A. J. (2020), 'Development of the 2017 national seismic hazard maps of Indonesia', *Earthquake Spectra* **36**(1), 112–136.  
**URL:** <https://doi.org/10.1177/8755293020951206>
- Irsyam, M., Hutabarat, D., Asrurifak, M., Imran, I., Widiyantoro, S., Hendriyawan, Sadisun, I., Hutapea, B., Afriansyah, T., Pindratno, H., Firmanti, A., Ridwan, M., Haridjono, S. W. and Pandhu, R. (2015), Development of seismic risk microzonation maps of Jakarta city, in 'Geotechnics for Catastrophic Flooding Events

- Proceedings of the 4th International Conference on Geotechnical Engineering for Disaster Mitigation and Rehabilitation (GEDMAR 2014)', pp. 35–47. January.

**URL:** <https://doi.org/10.1201/b17438-6>

Irsyam, M., Widiyantoro, S., Natawidjaja, D., Meilano, I., Rudyanto, A., Hidayati, S., Triyoso, W., Hanifa, N. R., Djarwadi, D., Faizal, L. and Sunarjito (2017), *Peta sumber dan bahaya gempa Indonesia tahun 2017*, Kementerian Pekerjaan Umum dan Perumahan Rakyat.

Kramer, S. L. and Stewart, J. P. (2024), *Geotechnical Earthquake Engineering. 2nd Editio, CRC Press. 2nd Edition*, Boca Raton: CRC Press.

Maheswari, R. (2024), 'Comparative Seismic Analysis of G+20 RC Framed Structure Building for with and without Shear Walls', *Journal of the Civil Engineering Forum* **10**(3), 257–266.

**URL:** <https://doi.org/10.22146/jcef.12854>

Marliyani, G. I., Arrowsmith, J. R. and Whipple, K. X. (2016), 'Characterization of slow slip rate faults in humid areas: Cimandiri fault zone, Indonesia', *Journal of Geophysical Research: Earth Surface* **121**(12), 2287–2308.

**URL:** <https://doi.org/10.1002/2016JF003846>

Pagani, M., Monelli, D., Weatherill, G., Danciu, L., Crowley, H., Silva, V., Henshaw, P., Butler, L., Nastasi, M. and Panzeri, L. (2014), 'OpenQuake engine: an open hazard (and risk) software for the global earthquake model', *Seismological Society of America*.

**URL:** <https://doi.org/10.1785/0220130087>

Scholz, C. H. (2019), *The Mechanics of Earthquakes and Faulting, 3rd Edition*, Cambridge: Cambridge University Press.

**URL:** <https://doi.org/10.1017/9781316681473>

Schwartz, D. P. and Coppersmith, K. J. (1984), 'Fault behavior and characteristic earthquakes: examples from the Wasatch and San Andreas fault zones (USA)', *Journal of Geophysical Research* **89**(B7), 5681–5698.

**URL:** <https://doi.org/10.1029/JB089iB07p05681>

Setiyono, U., Gunawan, I., Priyobudi, Yatimantoro, T., Imananta, R. T., Ramdhan, M., Hidayanti, Anggraini, S., Rahayu, R. H., Hawati, P., Yogaswara, D. S., Julius, A. M., Apriani, M., Harvan, M., Simangunsong, G. and Kriswinarso, T. (2019), *Katalog Gempabumi Signifikan dan Merusak 1821 - 2018*, Jakarta: Pusat Gempabumi

dan Tsunami Badan Meteorologi Klimatologi dan Geofisika.

Stirling, M., Gerstenberger, M., Litchfield, N., McVerry, G., Smith, W., Pettinga, J. and Barnes, P. (2008), 'Seismic hazard of the Canterbury Region, New Zealand: New earthquake source model and methodology', *Bulletin of the New Zealand Society for Earthquake Engineering* **41**(2), 51–67.

**URL:** <https://doi.org/10.5459/bnzsee.41.2.51-67>

Supendi, P., Winder, T., Rawlinson, N., Bacon, C. A., Palgunadi, K. H., Simanjuntak, A., Kurniawan, A., Widiyantoro, S., Nugraha, A. D., Shiddiqi, H. A., Ardianto, Daryono, Adi, S. P., Karnawati, D., Priyobudi, Marliyani, G. I., Imran, I. and Jatnika, J. (2023), 'A conjugate fault revealed by the destructive Mw 5.6 (November 21, 2022) Cianjur earthquake, West Java, Indonesia', *Journal of Asian Earth Sciences* **257**(July), 105830.

**URL:** <https://doi.org/10.1016/j.jseaes.2023.105830>

Wald, D. J. and Allen, T. I. (2007), 'Topographic slope as a proxy for seismic site conditions and amplification', *Bulletin of the Seismological Society of America* **97**(5), 1379–1395.

**URL:** <https://doi.org/10.1785/0120060267>

Widiyantoro, S., Irsyam, M., Faizal, L., Prakoso, W. A., Imran, I., Nazir, R., Soekarno, I., Wardani, S. P. R., Asrurifak, M., Sukamta, D., Hanifa, N. R., Djarwadi, D., Aldiamar, F., Hendarto, Alexander, N., Kadarman, J. S. and Rudyanto, A. (2022), *Peta Deagregasi Bahaya Gempa Indonesia Untuk Perencanaan dan Evaluasi Infrastruktur Tahan Gempa*, Jakarta: Kementerian Pekerjaan Umum dan Perumahan Rakyat.

Youngs, R. R. and Coppersmith, K. J. (1986), 'Implications of fault slip rates and earthquake recurrence models to probabilistic seismic hazard estimates', *International Journal of Rock Mechanics and Mining Sciences & Geomechanics Abstracts* **23**(4), 939–964.

**URL:** [https://doi.org/10.1016/0148-9062\(86\)90651-0](https://doi.org/10.1016/0148-9062(86)90651-0)

Zhao, J. X., Zhang, J., Asano, A., Ohno, Y., Oouchi, T., Takahashi, T., Ogawa, H., Irikura, K., Thio, H. K., Somerville, P. G., Fukushima, Y. and Fukushima, Y. (2006), 'Attenuation relations of strong ground motion in Japan using site classification based on predominant period', *Bulletin of the Seismological Society of America* **96**(3), 898–913.

**URL:** <https://doi.org/10.1785/0120050122>

[This page is intentionally left blank]